

**You might find this additional information useful...**

---

This article cites 15 articles, 10 of which you can access free at:

<http://jap.physiology.org/cgi/content/full/90/6/2088#BIBL>

This article has been cited by 17 other HighWire hosted articles, the first 5 are:

**Neither fibrin nor plasminogen activator inhibitor-1 deficiency protects lung function in a mouse model of acute lung injury**

G. B. Allen, M. E. Cloutier, Y. C. Larrabee, K. Tetenev, S. T. Smiley and J. H. T. Bates  
*Am J Physiol Lung Cell Mol Physiol*, March 1, 2009; 296 (3): L277-L285.

[Abstract] [Full Text] [PDF]

**Ventilator-induced Lung Injury Distribution: The Key to Understanding Injury Mechanisms**

S. Tsuchida and B. P. Kavanagh  
*Am. J. Respir. Crit. Care Med.*, January 1, 2007; 175 (1): 96-96.

[Full Text] [PDF]

**Quantification of atelectatic lung volumes in two different porcine models of ARDS**

J. Karmrodt, C. Bletz, S. Yuan, M. David, C.-P. Heussel and K. Markstaller  
*Br. J. Anaesth.*, December 1, 2006; 97 (6): 883-895.

[Abstract] [Full Text] [PDF]

**Cellular Stress Failure in Ventilator-injured Lungs**

N. E. Vlahakis and R. D. Hubmayr  
*Am. J. Respir. Crit. Care Med.*, June 15, 2005; 171 (12): 1328-1342.

[Abstract] [Full Text] [PDF]

**Acoustic evidence of airway opening during recruitment in excised dog lungs**

Z. Hantos, J. Tolnai, T. Asztalos, F. Petak, A. Adamicza, A. M. Alencar, A. Majumdar and B. Suki

*J Appl Physiol*, August 1, 2004; 97 (2): 592-598.

[Abstract] [Full Text] [PDF]

Medline items on this article's topics can be found at <http://highwire.stanford.edu/lists/artbytopic.dtl> on the following topics:

Physiology .. Lungs  
Physiology .. Pulmonary Alveoli  
Medicine .. Airway  
Medicine .. Lung Capacity  
Chemistry .. Surface Tension  
Veterinary Science .. Dogs

Updated information and services including high-resolution figures, can be found at:

<http://jap.physiology.org/cgi/content/full/90/6/2088>

Additional material and information about *Journal of Applied Physiology* can be found at:

<http://www.the-aps.org/publications/jappl>

---

This information is current as of November 11, 2009 .

# Mechanics of edematous lungs

THEODORE A. WILSON,<sup>1</sup> RON C. ANAFI,<sup>1</sup> AND ROLF D. HUBMAYR<sup>2</sup>

<sup>1</sup>Department of Aerospace Engineering and Mechanics, University of Minnesota, Minneapolis 55455; and <sup>2</sup>Division of Pulmonary and Critical Care Medicine, Mayo Clinic and Foundation, Rochester, Minnesota 55409

Received 23 August 2000; accepted in final form 9 January 2001

**Wilson, Theodore A., Ron C. Anafi, and Rolf D. Hubmayr.** Mechanics of edematous lungs. *J Appl Physiol* 90: 2088–2093, 2001.— Using the parenchymal marker technique, we measured pressure (P)-volume (P-V) curves of regions with volumes of  $\sim 1$  cm<sup>3</sup> in the dependent caudal lobes of oleic acid-injured dog lungs, during a very slow inflation from P = 0 to P = 30 cmH<sub>2</sub>O. The regional P-V curves are strongly sigmoidal. Regional volume, as a fraction of volume at total lung capacity, remains constant at 0.4–0.5 for airway P values from 0 to  $\sim 20$  cmH<sub>2</sub>O and then increases rapidly, but continuously, to 1 at P =  $\sim 25$  cmH<sub>2</sub>O. A model of parenchymal mechanics was modified to include the effects of elevated surface tension and fluid in the alveolar spaces. P-V curves calculated from the model are similar to the measured P-V curves. At lower lung volumes, P increases rapidly with lung volume as the air-fluid interface penetrates the mouth of the alveolus. At a value of P =  $\sim 20$  cmH<sub>2</sub>O, the air-fluid interface is inside the alveolus and the lung is compliant, like an air-filled lung with constant surface tension. We conclude that the properties of the P-V curve of edematous lungs, particularly the knee in the P-V curve, are the result of the mechanics of parenchyma with constant surface tension and partially fluid-filled alveoli, not the result of abrupt opening of airways or atelectatic parenchyma.

pressure-volume curve; surface tension; regional ventilation; acute lung injury

IN NORMAL LUNGS, FLUID THAT permeates through the capillary walls is carried off by the lymphatic system, the lung is maintained in a relatively dry state, and interstitial pressures are negative. If pressure in the capillaries increases or capillary permeability increases, the fluid balance for the lung may be disrupted. In that case, fluid first accumulates in the interstitium and then enters the alveolar space. Proteins in the fluid disrupt normal surfactant function, gas exchange is impaired, and the pressure-volume (P-V) behavior of the lung is altered. The management of ventilation in patients with pulmonary edema is a significant medical concern. At this point, the physiology of edema and the mechanics of edematous lungs are not fully understood.

The dominant current concept of the mechanics of edematous lungs is based on interpretations of computerized tomography scans and P-V curves. From these

data, it has been inferred that dependent regions of edematous lungs collapse at lower transpulmonary pressures and that they reopen abruptly at an elevated opening pressure (4, 5, 8). Martynowicz et al. (9) reported the first direct measurements of regional volume in edematous lungs. They used the parenchymal marker technique to measure regional volume during tidal ventilation in dog lungs after oleic acid (OA) injury. In this technique, 12–15 radiopaque markers are placed in the thick, dorsal region of a caudal lobe, the three-dimensional positions of the markers are obtained from biplane fluoroscopic images, and the volumes of tetrahedra with markers as vertices are computed. With the dog in the supine position, the markers lie in the dependent part of the lung. For tidal ventilation with small values of positive end-expiratory pressure (PEEP), regional volumes in this region of the injured lungs were found to be somewhat larger than regional volume at the same airway pressure in the control state before injury, but regional ventilation was much smaller than that in the control state. Values of PEEP of 15 cmH<sub>2</sub>O were required to restore regional ventilation to control values (10). The data for regional volume as a function of time were searched for evidence of abrupt opening, but none was found. These results are contrary to the idea that the dependent lung is atelectatic at lower transpulmonary pressures and reopens abruptly at a critical opening pressure.

Here we report data on regional volume in injured lungs for a different maneuver: a slow inflation from a small initial airway pressure to P > 30 cmH<sub>2</sub>O [total lung capacity (TLC)]. We find that the P-V curves of dependent regions of injured lungs are strongly sigmoidal. At low airway pressures, regional volumes range from 40 to 50% of regional volume at TLC. These regions change volume very slowly until airway pressure reaches  $\sim 20$  cmH<sub>2</sub>O. Regional volumes then increase rapidly to TLC. These data are consistent with regional lung behavior during mechanical ventilation. At lower airway pressures, regional volume is high, but regional compliance is low. At higher airway pressures, regional compliance is higher than control.

We also present a model for the mechanics of edematous lungs. A model alveolus is described. The param-

Address for reprint requests and other correspondence: T. A. Wilson, 107 Akerman Hall, 110 Union St. SE, Minneapolis, MN 55455 (E-mail: wilson@aem.umn.edu).

The costs of publication of this article were defrayed in part by the payment of page charges. The article must therefore be hereby marked "advertisement" in accordance with 18 U.S.C. Section 1734 solely to indicate this fact.

eters of the model are chosen so that the model matches data from the literature on the dependence of alveolar surface area on lung V and surface tension. The model is then modified to represent the edematous lung by assuming that surface tension is constant in the edematous lung and that the alveolus is partially filled with fluid. P-V curves are calculated from the model. The model P-V curves are similar to the measured P-V curves: lung compliance is low at lower P values and increases abruptly at transpulmonary pressures of  $\sim 20$  cmH<sub>2</sub>O. Thus we conclude that the mechanical properties of edematous lungs can be explained without recourse to alveolar collapse and reopening or airway closure and reopening. These features of the P-V curve of the edematous lung are the result of internal stresses in the lung that are caused by high surface tension and the presence of fluid in the lung.

### EXPERIMENTAL METHODS

To measure regional lung expansion during mechanical ventilation, the parenchymal marker technique was used. It has been described in detail previously (7). Briefly, 1-mm metal beads were implanted transthoracically into the caudal lobe of two anesthetized dogs. Nine weeks later, experiments were conducted during which biplane fluoroscopic images of the thorax were recorded on videotape. The orthogonal projection images of each bead were sampled at the rate of 5 Hz using an operator-interactive computer tracking system. The three-dimensional marker locations were derived from these data. Four markers define a volume (tetrahedron) that contains air, tissue, edema fluid, and blood. Thus, as a final output, the method provides the description of regional volume behavior in time (i.e., regional spirometry).

All techniques and procedures were approved by Mayo's Institutional Animal Care and Use Committee, and the care and handling of the animals were in accordance with National Institutes of Health guidelines. Two adult,  $\approx 10$ -kg beagle dogs were studied. The animals were anesthetized with pentobarbital sodium (30 mg/kg, with supplemental doses of 10 mg/h), a tracheostomy was performed, and a 9-mm ID glass cannula was inserted into the tracheal lumen. The dogs were mechanically ventilated (Servo 900C, Siemens, Solna, Sweden) with a fractional oxygen concentration of 1.0, a tidal volume of 230–250 ml, a respiratory rate of 20 cycles/min, an inspiratory time fraction of 0.33, and a PEEP set between 3 and 5 cmH<sub>2</sub>O. Airway opening pressure (P) was measured at the proximal end of the endotracheal tube

(24A1, Honeywell Microswitch, Freeport, IL). Gas flow rates were measured by using a pneumotachograph and transducer (163PC, Honeywell, Microswitch) attached to the Y piece of the ventilator circuit. Flow was integrated to monitor the tidal volume. A pediatric Swan-Ganz pulmonary arterial catheter was inserted through the right internal jugular vein to monitor pulmonary arterial pressure. Systemic blood pressure was monitored from the femoral arterial line with a pressure transducer (P37A, Statham, Oxnard, CA). Three leads attached to the paws provided a single electrocardiographic tracing to monitor the heart rate. Body temperature was monitored rectally (Tele-thermometer 44TF, Yellow Springs Instruments, Yellow Springs, OH) and kept constant at 37°C using heat lamps. A 16-F cannula was placed in a peripheral vein to administer normal saline and anesthetic. Normal saline was administered to maintain hemodynamic stability. Airway opening pressure, gas flow, and notes taken during the experiment were stored in a digital form (Lab-View, National Instruments, Austin, TX).

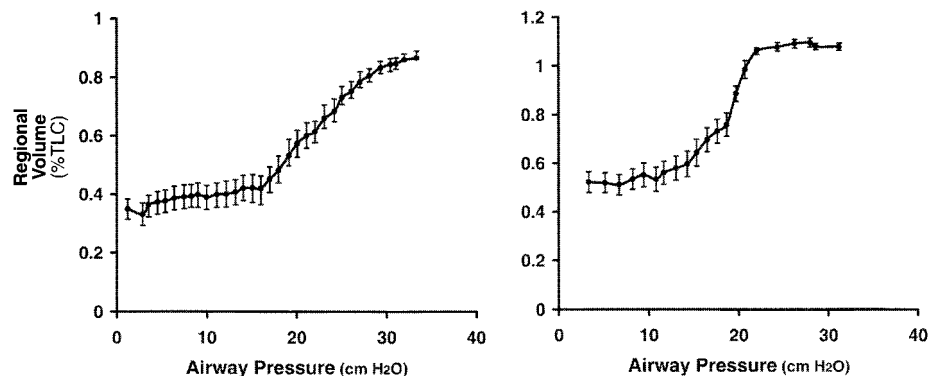
The animals were paralyzed with pancuronium bromide (3 mg iv), and their inspiratory capacity was determined by inflating the lungs to an airway pressure of 35 cmH<sub>2</sub>O. The thorax was imaged at TLC so that postinjury measurements of regional lung expansion could later be normalized by preinjury lung dimensions at TLC. After this baseline measurement, the animals were turned prone and injected with 0.09 ml/kg OA in three aliquots via the right atrial port of the pulmonary arterial catheter. Animals were repositioned supine 5 min after the last OA injection. Approximately 3 h after the OA injection, the animals were disconnected from the ventilator circuit, and the lungs were imaged while the thorax was inflated with a constant flow of  $<5$  ml/s to  $P > 40$  cmH<sub>2</sub>O (Harvard Apparatus, Cambridge, MA). Because this maneuver lasted for up to 5 min, both animals died during the slow inflation.

### RESULTS

Figure 1 shows the average regional volume-airway pressure curves of two OA-injured dogs. Each data point represents the mean  $\pm$  SD of the volumes of 10 minimally overlapping tetrahedra. The curves show similar features: regional volume nearly constant for  $P < 15$  cmH<sub>2</sub>O, a knee at P between 15 and 20 cmH<sub>2</sub>O, a steep (compliant) midportion between 20 and 25 cmH<sub>2</sub>O, and a plateau at  $P > 25$ –30 cmH<sub>2</sub>O.

We should note that we did not attempt to measure esophageal pressure in these experiments because we do not have confidence that esophageal pressure is representative of pleural pressure for the edematous

Fig. 1. Regional pressure-volume curves of tetrahedra in dependent regions of 2 lungs after oleic acid injury. Values are averages  $\pm$  SD of volumes, as a fraction of total lung capacity (TLC), of 10–15 nonoverlapping tetrahedra. Absolute volumes of the tetrahedra at TLC ranged from 1 to 2 cm<sup>3</sup>.



lungs. As a result, the experimental results describe regional volume as a function of airway opening pressure, and these results will be compared with the results of a model that describes regional volume as a function of transpulmonary pressure. However, we would expect pleural pressure to increase with increasing  $V$ . Therefore, transpulmonary pressure would increase less rapidly with increasing  $V$  than would airway opening pressure, and the compliant regions of the curves would occur at somewhat lower pressures and be somewhat steeper than those shown in Fig. 1.

## MODEL

In the late 1970s, Weibel and colleagues (1, 6) at Berne reported systematic data on the morphology of rabbit lungs at different  $V$  values and for different values of surface tension. Guided by Weibel's (15) description of the architecture of the lung, the qualitative appearance of the micrographs, and the quantitative data, Wilson and Bachofen (16) constructed a model for the mechanical properties of the acinus. The model alveolar duct consisted of intersecting helical elastic line elements that defined the lumen of the duct and formed the free edges of alveolar walls that extended outward from the helical line elements. The alveolar walls were assumed to carry no tissue stress and to serve only as platforms for surface tension at the air-liquid interface. Tension and length of the line elements were determined by a balance between the hoop stress in the line and surface tension on the alveolar walls. The model fit the data well.

Here we describe a modified version of this model. Instead of modeling the alveolar duct, we model an alveolus. The model of a representative alveolus is shown in Fig. 2. First, we focus on the model for the normal air-filled lung, shown in Fig. 2, *left*. The model is axisymmetric around the vertical axis in Fig. 2. The sides of the alveolus have the shape of the frustrum of a cone with cone angle  $\alpha$ . The wide end of the cone is capped by a spherical segment that meets the sides at an angle of  $120^\circ$ . The bottom of the frustrum is open to the alveolar duct. The vertex of the cone is situated on the centerline of the alveolar duct. The volume of the alveolus plus the part of the alveolar duct associated with each alveolus is denoted  $v$ . Thus  $v$  equals the volume of the entire figure from the vertex to the cap. In the normal air-filled lung, the surface area of the air-liquid interface ( $s$ ) is the inner surface of the frustrum and cap. The distance from the vertex to the top of the cone ( $h$ ) is assumed to increase with the cube root of  $V$ . That is,  $h = h_0 (v/v_0)^{1/3}$ , where  $h_0$  is a constant and  $v_0$  is alveolar volume for  $h = h_0$ . The distance along the generatrix of the cone from the vertex to the entrance ring at the mouth of the alveolus is denoted  $r$ . Thus surface area can be written as the difference between the surface area of the entire cone and cap ( $s_1$ ), which depends on  $h$  only, and the missing surface area between the apex and the alveolar wall

$$s = s_1(h) - \pi r^2 \sin \alpha \quad (1)$$

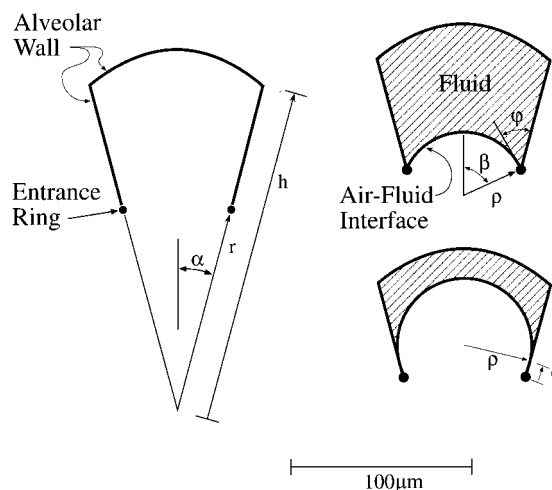


Fig. 2. Model alveolus. *Left*: the model alveolus consists of the frustrum of a cone with cone angle  $\alpha$  and a spherical cap. The spherical cap meets the side of the cone at an angle of  $120^\circ$ . The vertex of the cone lies on the axis of the alveolar duct, and distance  $h$  from the vertex to the top of the cone increases with the cube root of lung volume. An elastic line element forms the entrance ring at the alveolar opening. The distance  $r$  from the vertex to the entrance ring depends on a balance between hoop stress in the elastic line and the outward pull of surface tension. *Right*: the geometry of the alveolus in the edematous lung is shown. *Top*: for case 1, the air-fluid interface is anchored at the entrance ring. The interface is a spherical surface with radius  $\rho$ . The angle between the axis and the radius to the entrance ring is denoted  $\beta$ , and the angle between the tangent to the surface and the alveolar wall is denoted  $\phi$ . *Bottom*: for case 2, the bubble has penetrated the alveolus, and the spherical air-liquid interface is tangent to the wall and meets the wall as a distance  $q$  above the entrance ring. The dimensions shown in all figures are for lung volume of 60% TLC. *Left*: normal air-filled lung; *right*: edematous lungs with fluid volumes of 40 (top) and 20% TLC (bottom).

An elastic line element forms the entrance ring and supports the free edge of the alveolar wall. The length  $L$  of the line element is  $2\pi r \sin \alpha$ . Tension ( $T$ ) in this line element is a function of the ratio of its length  $L$  to its unstressed length  $L_0$ . Because  $L$  is proportional to  $r$ ,  $L/L_0 = r/r_0$ , where  $r_0$  is the value of  $r$  for which the line element is unstressed. The tension-length behavior of the line element is described by Eq. 2 where  $A$  and  $a$  are constants

$$T = A(r/r_0 - 1) \exp[a(r/r_0 - 1)^2] \quad (2)$$

Surface tension  $\gamma$  at the air-liquid interface pulls outward on the entrance ring. As the ring expands, surface area decreases, and tension and length of the line element increase. Static equilibrium occurs at the length at which the sum of the surface energy and elastic energy stored in the line element is minimum. That is, the equilibrium value of  $r$  is determined by the equation

$$\gamma ds/dr + TdL/dr = 0 \quad (3)$$

By substituting Eq. 1 and the expression for  $L$  into Eq. 3, we obtain the relation

$$T = \gamma/r \quad (4)$$

This equation is recognized as the balance between the outward pull of surface tension and the inward hoop

stress in a line carrying tension  $T$  with curvature  $r$ . Thus, to obtain a self-consistent mechanistic model of the alveolus, the radius of curvature of the elastic line element must be taken to be  $r$ . The length of the line element associated with one alveolus is the length of the entrance ring, but this ring must be pictured as being made up of segments of rings that run around the axis of the duct.

Our objective is to use the model to calculate recoil pressure for the lung. The model for the relation between whole lung properties and alveolar properties is the same as the model we have used before. Recoil of the lung ( $P$ ) is assumed to be the result of tension in connective tissue in the lung and surface tension at the air-liquid interface. The connective tissue system has two components (15). The first is the peripheral tissue system consisting of the pleural membrane, the bronchial tree, and interlobular membranes that connect the pleural membrane to the bronchial tree to form a connected structure. The stress in this component depends on  $V$  only and provides the recoil of the saline-filled lung. Its contribution to recoil is, therefore, denoted  $P_{sal}$ . The second tissue component is the axial tissue system, the system of elastic line elements that form the alveolar openings. As described above, these elements are extended by surface tension. Finally, surface tension contributes directly to recoil, as well as contributes indirectly through its effect on the axial tissue system.

Two relations between recoil and alveolar properties can be invoked. The first is the energy balance in which the incremental work of lung inflation for an incremental volume change ( $dV$ ) is set equal to the change in energy of the tissue and the air-liquid interface. The incremental energy stored in the peripheral tissue system is  $P_{sal}dV$ , and the incremental energies stored in the axial tissue system and interface are the incremental energies for an alveolus multiplied by the number of alveoli, denoted  $n$ .

$$PdV = P_{sal}dV + n\gamma ds + nTdL \quad (5)$$

Alternatively, recoil can be calculated from a force balance for a plane cut through the parenchyma. Here,  $P$  acts in one direction on the plane, the tissue and surface forces act in the opposite direction, and these must balance the pressure force. The tissue line elements and air-liquid interfaces of the lung are assumed to be randomly oriented. It follows that the force balance has the following form (16)

$$P = P_{sal} + \frac{2}{3}\gamma ns/V + \frac{1}{3}nT/V \quad (6)$$

For the model to be consistent, *Eqs. 5* and *6* must give the same values of  $P$ , and, with  $T$  related to  $r$  by *Eq. 4*, they are consistent, and either can be used to calculate  $P$ .

The value of  $n$  is obtained by dividing  $V$  at TLC by  $v_0$ . Then  $P$  and total lung surface area ( $S$ ) can be calculated from *Eqs. 1, 2, 4, and 6*. Parameter values were chosen to match the calculated values of  $P$  and  $S$  for different  $V$  values and values of surface tension (12) to values reported in the literature for rabbit lungs (1, 6).

These values are as follows:  $\alpha = 15^\circ$ ,  $h_0 = 250 \mu\text{m}$ ,  $r_0 = 100 \mu\text{m}$ ,  $A/r_0 = 60 \text{ dynes/cm}$ , and  $a = 2.5$ .

The model for the alveolus in the edematous lung is shown in Fig. 2, *right*. The fluid is assumed to form a pool at the back of the alveolus. The air-fluid interface is a segment of a sphere with radius  $\rho$ . Two cases are possible. In the first, fluid covers the alveolar walls completely, and the air-fluid interface extends to the entrance ring. The angle between the tangent to the air-liquid interface at its edge and the alveolar wall is denoted  $\phi$ , and the angle between the perpendicular to the air-fluid interface at its edge and the axis of the alveolus is denoted  $\beta$ . Thus  $\phi = \pi/2 + \alpha - \beta$  and  $\rho = r \sin \alpha / \sin \beta$ . In the second case, the fluid pool is inside the alveolus, and the air-fluid interface meets the alveolar wall at a distance  $q$  from the apex of the cone. The air-liquid interface is tangent to the wall at the wall, and  $\phi = 0$  in this case.

The energy balance and the force balance are altered when fluid occupies a significant fraction of  $V$ . First, we divide  $V$  into two parts,  $V_{air}$  and  $V_f$ , denoting the volumes of air and fluid, respectively. Pressure in the air is  $P$ , and pressure in the fluid is denoted  $P_f$ . The energy balance has the form

$$PdV_{air} + P_f dV_f = P_{sal}(dV_{air} + dV_f) + n\gamma ds + nTdL \quad (7)$$

The force balance equation is also altered. The fraction of a plane through the lung occupied by air is  $V_{air}/V$ , and the fraction occupied by fluid is  $V_f/V$ . Therefore, the force balance is as follows

$$P(V_{air}/V) + P_f(V_f/V) = P_{sal} + \frac{2}{3}n\gamma s/V + \frac{1}{3}nTL/V \quad (8)$$

With the following relations between the variables, these two equations are consistent for all values of  $V_{air}$  and  $V_f$

$$P_f = P_{sal}, P = P_f + 2\gamma/\rho, T = \gamma \cos \phi/r \quad (9)$$

The second of these is the usual equation for the pressure difference across a spherical surface with surface tension  $\gamma$  and radius  $\rho$ . The third is similar to *Eq. 4* with the radial component of  $\gamma$  balancing the hoop stress in the line element.

The calculation of  $P$ - $V$  curves for the edematous lung is quite simple. The value of  $\gamma$  was assumed to be  $36 \text{ dyn/cm}$  in the edematous lung. For *case 1*, for values of  $\beta$  from  $\beta = \alpha$  to  $\beta = \pi/2 + \alpha$ , the  $V_{air}$  was computed for the geometry shown in the Fig. 2, *top right*,  $r$  was obtained from the solution of the third of *Eqs. 9* and *2*, and  $\rho$  was obtained from  $r$ . Then  $P$  was computed from the equation

$$P = P_{sal} + 2\gamma/\rho$$

where  $P_{sal}(V)$  is taken from data in the literature. Similarly for *case 2*, for values of  $q$  beginning with  $q = 0$ , the  $V_{air}$  was computed for the geometry shown in Fig. 2, *bottom right*, and the calculation of  $P$  follows as that for *case 1*.

Calculated P-V curves for edematous lungs with different amounts of fluid are shown in Fig. 3. These curves begin at values of P and V for which  $\beta = \alpha$ . At this point, the line elements are unstressed, and P is higher than  $P_{sal}$  because of the surface tension at the air-liquid interface. Although surface tension is high, the area of the air-liquid interface is small, and P is  $\sim 7$  cmH<sub>2</sub>O greater than  $P_{sal}$ . As V increases, the air bubble penetrates the mouth of the alveolus, surface area increases, and the line elements are stretched. As a result, P increases rapidly with V. At the points marked by arrows,  $\phi = 0$ . At higher values of V, the air-liquid interface retreats into the alveolus, surface area increases, but the tension in the line elements remains constant. These segments of the P-V curve are like those of lungs that have been rinsed with a fluid with high surface tension.

## DISCUSSION

Our laboratory's previous measurements of the volume of dependent regions of OA-injured lungs during tidal volume oscillations showed that regional volume was somewhat higher than regional volume in normal lungs at the same transpulmonary pressure and that tidal volume was much smaller than normal (9). The observation that regional volume was high was contrary to the concept that dependent regions were collapsed in edematous lungs. We also observed no evidence of discontinuous opening of regions, and this is also contrary to the concept that airways and atelectatic parenchyma pop open at some critical opening pressure. Our

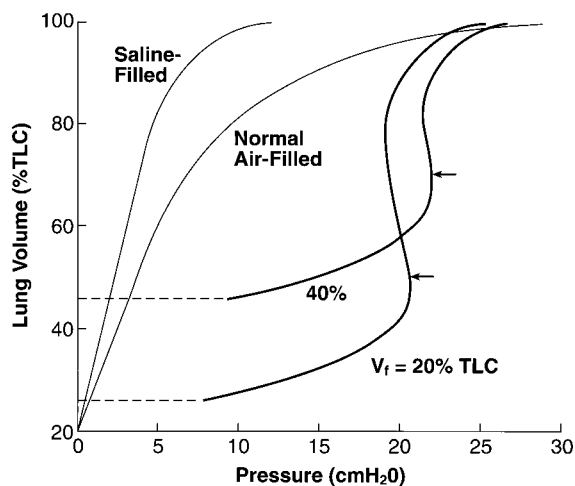


Fig. 3. Pressure-volume curves for saline-filled, normal air-filled, and edematous lungs with fluid volumes ( $V_f$ ) of 20 and 40% TLC. The curve for saline-filled lungs is taken from the literature (6). The curve for the normal air-filled lung is calculated from the model, using values of surface tension vs. lung volume from the literature (12). The curves for the edematous lung are calculated from the model. For pressures  $< 8$  cmH<sub>2</sub>O (dashed line), the duct is assumed to be blocked by liquid bridges. Calculated values are shown by solid lines. Arrows show the point of transition between the geometry shown in Fig. 2, *top right*, and the geometry shown in the *bottom right*. As the air bubble penetrates the mouth of the alveolus, pressure rises rapidly, and lung compliance is low. The segment of the curve with the air bubble within the alveolus is like those for lungs rinsed with a fluid with constant surface tension (13, 14), and lung compliance is high.

motivation for measuring regional volume during a very slow inflation of dependent regions of edematous lungs was to search for evidence of abrupt opening of atelectatic regions. In these experiments, we, therefore, covered the entire range of P values from 0 to 30 cmH<sub>2</sub>O, and we inflated slowly so that popping at a critical value of P would be more evident in the trace of volume vs. time. To be sure, the resolution of the technique is limited. Popping of regions much smaller than 1 cm<sup>3</sup> might not be apparent in our data. However, taken at face value, the data show no evidence of abrupt opening. In addition, these data for slow inflation are consistent with the data for tidal volume oscillations; regional volume is elevated at lower P values, and regional compliance is very low for P values  $< 20$  cmH<sub>2</sub>O. In addition, in these experiments, we reached values of P at which dependent regions expanded. The expansion yields a knee in the P-V curve. The rise in volume is sharp but continuous. Thus the data for the full inflation P-V behavior support our contention that the concept of atelectasis and abrupt opening of dependent regions in edematous lungs is incorrect.

The very compliant part of the P-V curve at high P values reminded us of the behavior of lungs in which surface tension had been altered by rinsing of the lungs with fluids with fixed surface tension (13). That behavior has been modeled successfully (14). Edema is known to alter surface tension, and thus the part of the P-V curve at higher volumes and higher P values seemed to be explainable by established ideas about parenchymal mechanics. On the other hand, a significant amount of fluid in the parenchyma might be expected to reduce the area of the air-fluid interface and reduce recoil. We, therefore, sought to describe the transition from the fluid-filled to the air-filled, high-surface-tension state.

The model that is described in this paper is a modified version of an earlier model. The earlier model successfully described the dependence of lung recoil and surface area on V and surface tension. In that model, the line elements at the alveolar openings were pictured as helices. Alveolar walls extended radially outward from the helices, but the geometry of the alveolus was not specified. Here, we have modified that model by describing the alveolar geometry in detail. This detail was required to add fluid to the model. By modeling the side walls of the alveolus as a cone, the geometry of the fluid pool and the air-liquid interface could be described simply. However, this model is not as self-consistent as the earlier model. In particular, it is not possible to match a model of an alveolus with cylindrical symmetry around a vertical axis to a model of a duct with cylindrical symmetry around a horizontal axis. That is, identical model alveoli cannot be joined to produce a model duct. The model alveolus must be considered to represent the average geometry of the alveolus.

Although the modified model is less satisfactory than the original in some ways, it retains the crucial elements of the original. These elements are as follows. The dimensions of the outer boundary of the duct depend on V alone. Tension and length of the line

element at the inner boundary are determined by a balance between hoop stress and surface tension. Surface area is a function of both outer and inner dimensions and depends on both  $V$  and surface tension.

In the model for edema, the fluid in the lung was assumed to be confined to the interior of the alveolus. This assumption is consistent with the micrographs of edematous lungs presented by Bachofen et al. (2). In these micrographs, the alveolar ducts and alveolar mouths are open, and the alveolar walls are separate and distinct. With smaller amounts of edema fluid, the fluid is confined to the interior corners of the alveoli. With larger amounts of fluid, the fluid pools extend to the free edges of the alveolar walls, and the air-liquid interfaces are smoothly curved. There are no signs of alveolar collapse and atelectasis. Because the section of lung that is shown in a micrograph cuts different alveoli at different depths and different angles, it is difficult to tell whether the fluid is uniformly distributed among the alveoli or not. Our analysis of a single alveolus implies the assumption that the fluid is approximately uniformly distributed among alveoli.

The results of the calculation of P-V curves for the model of edematous lungs are shown in Fig. 3. The calculated values begin at a P of  $\sim 8$  cmH<sub>2</sub>O. At that point the alveolus is filled with fluid, and the entrance ring is unstressed. For lower volumes and P values, the fluid would bulge into the alveolar duct, and the entrance ring would be compressed. This state is unstable. The stability of a fluid layer on the wall of an airway has been analyzed (3, 11). The results show that, roughly speaking, if enough fluid is available to form a liquid bridge across the airway, the bridge will form. Thus we think that, at lower volumes, bridges would form across the duct and block flow, and the horizontal dashed lines in Fig. 3 represent this assumption that the airways are blocked at lower volumes and P values. As volume increases above the minimum volume, the air bubble is forced into the alveolus, and surface area and tension in the line element increase rapidly. In this range of P values, P increases rapidly as V increases, and lung compliance is small. At high volumes, the P-V curve is nearly vertical as it is for lungs that have been rinsed with a liquid with high surface tension (13). This model, like other existing models, predicts a negative slope for the P-V curve for constant surface tension. If surface tension is constant and surface area increases with the  $V^{2/3}$ , the second term on the right side in Eq. 6 decreases as V increases. This aspect of the P-V curve of lungs with constant surface tension is discussed by Stamenovic and Smith (14).

In Fig. 3, we show calculated P-V curves for  $V_f$  values of 20 and 40% TLC. The  $V_f$  in injured lungs is unknown, and it is not certain that the amount of fluid remained constant as the lungs were inflated. Thus the amount of fluid and the assumption that the  $V_f$  remains constant must be added to the other assumptions in the model.

Nonetheless, with the assumptions that were made, the model yields P-V curves that are similar to the measured curves. Thus the model explains the low compliance of edematous lungs at lower P values, the knee in the P-V curve at transpulmonary pressures of  $\sim 20$  cmH<sub>2</sub>O, and the high compliance at higher P values. These properties are the result of a transition from fluid-filled alveoli to air-filled alveoli with constant surface tension. The alveolar tissue is fully opened during this transition. This explanation for the knee of the P-V curve is quite different from the explanation that is based on the hypothesis that the alveoli or airways are collapsed and pop open at a critical P.

This work was supported by National Heart, Lung, and Blood Institute Grant HL-57364.

## REFERENCES

1. **Bachofen H, Gehr P, and Weibel ER.** Alterations of mechanical properties and morphology in excised rabbit lungs rinsed with a detergent. *J Appl Physiol* 47: 1002–1010, 1979.
2. **Bachofen H, Schurch S, Michel RP, and Weibel ER.** Experimental hydrostatic pulmonary edema in rabbit lungs. *Am Rev Respir Dis* 147: 989–996, 1993.
3. **Cassidy KJ, Halpern D, Ressler BG, and Grotberg JB.** Surfactant effects in model airway closure experiments. *J Appl Physiol* 87: 415–427, 1999.
4. **Gattinoni L, Pelosi P, Crotti S, and Valenza D.** Effects of positive end-expiratory pressure on regional distribution of tidal volume and recruitment in adult respiratory distress syndrome. *Am J Respir Crit Care Med* 151: 1807–1814, 1995.
5. **Gattinoni L, Pesenti A, Avalli L, Rossi F, and Bombino M.** Pressure-volume curve of total respiratory system in acute respiratory failure: computed tomographic scan study. *Am Rev Respir Dis* 136: 730–736, 1987.
6. **Gil J, Bachofen H, Gehr P, and Weibel ER.** The alveolar volume to surface area relationship in air- and saline-filled lungs fixed by vascular perfusion. *J Appl Physiol* 47: 990–1001, 1979.
7. **Hubmayr RD, Walters BJ, Chevalier PA, Rodarte JR, and Olson LE.** Topographical distribution of regional volume in anesthetized dogs. *J Appl Physiol* 54: 1048–1056, 1983.
8. **Lachmann B.** Open up the lung and keep the lung open. *Intensive Care Med* 18: 319–321, 1992.
9. **Martynowicz MA, Minor TA, Walters BJ, and Hubmayr RD.** Regional expansion of oleic acid-injured lungs. *Am J Respir Crit Care Med* 160: 250–258, 1999.
10. **Martynowicz MA, Wilson TA, Walters BJ, and Hubmayr RD.** Effects of PEEP and posture on regional recruitment of oleic acid injured lungs in situ (Abstract). *Am J Respir Crit Care Med* 159: A479, 1999.
11. **Otis DR, Johnson M, Pedley TJ, and Kamm RD.** Role of pulmonary surfactant in airway closure: a computational study. *J Appl Physiol* 75: 1323–1333, 1993.
12. **Schurch S, Goerke J, and Clements J.** Direct determination of volume- and time-dependence of alveolar surface tension in excised lungs. *Proc Natl Acad Sci USA* 73: 4698–4702, 1978.
13. **Smith JC and Stamenovic D.** Surface forces in lungs. Alveolar surface tension-lung volume relationships. *J Appl Physiol* 60: 1341–1350, 1986.
14. **Stamenovic D and Smith JC.** Surface forces in lungs. II. Microstructural mechanics and lung stability. *J Appl Physiol* 60: 1351–1357, 1986.
15. **Weibel ER.** Functional morphology of lung parenchyma. In: *Handbook of Physiology. The Respiratory System. Mechanics of Breathing.* Bethesda, MD: Am. Physiol. Soc., 1986, sect. 3, vol. III, pt. 1, chapt. 8, p. 89–112.
16. **Wilson TA and Bachofen H.** A model for mechanical structure of the alveolar duct. *J Appl Physiol* 52: 1064–1070, 1982.